MARCH 1985 LRP 249/84

BUFFER GASES TO INCREASE THE EFFICIENCY OF AN OPTICALLY PUMPED FAR INFRARED D_2O LASER

R. Behn, M.-A. Dupertuis, I. Kjelberg,
P.A. Krug, S.A. Salito and M.R. Siegrist

BUFFER GASES TO INCREASE THE EFFICIENCY OF AN OPTICALLY PUMPED FAR INFRARED D_2O LASER

R. Behn, M.-A. Dupertuis, I. Kjelberg,
P.A. Krug, S.A. Salito and M.R. Siegrist

Centre de Recherches en Physique des Plasmas
Association Euratom - Confédération Suisse
Ecole Polytechnique Fédérale de Lausanne
21, av. des Bains - 1007 Lausanne/Switzerland

ABSTRACT

The effects of buffer gas additives on the performance of an optically pumped D_2O laser operating at 385 μm have been investigated both experimentally and by numerical simulation. Three gases, sulphur hexafluoride, carbon tetrafluoride and n-hexane were found to produce an increase of up to 40% in the pumping efficiency, as well as significant lengthening of the far infrared pulse. Under optimum conditions 2.6 J in a 1 μs long pulse have been obtained.

The buffer gases are shown to eliminate the vibrational deexcitation bottleneck, which in pure D_2O leads to an accumulation of population in the upper vibrational level, and hence a reduction in the efficiency of absorption of the pump beam.

Comparison of the observed buffer gas effects with the predictions of a numerical simulation code based on a rate equation model gives information about the constants for vibrational and rotational relaxation rates due to D_2O-D_2O and D_2O-buffer gas collisions.

I. INTRODUCTION

The development of a high power far infrared (FIR) D_2O laser is mainly motivated by its application to plasma diagnostics. In order to measure the ion temperature of a tokamak plasma by collective Thomson scattering of FIR radiation we require a laser source that is capable of producing 1 MW in a pulse of at least 1 μs duration. The optically pumped D_2O laser emitting on the 385 μm line has been chosen because it delivers sufficiently powerful output at a wavelength where sensitive detectors are available.

Although the megawatt power level has already been reached for shorter pulses (about 150 ns) [1], high power operation is more difficult to obtain for pulse lengths exceeding 0.5 μs. The mechanism preventing efficient long pulse operation is a bottleneck in the vibrational deexcitation which hinders recycling of D_2O molecules to the ground state. The depletion of ground state population reduces pump beam absorption and thus leads to a decrease in efficiency of the FIR laser.

Pump saturation can be avoided if the pump beam power density can be reduced by increasing the cross section of the active volume of the D_2O laser. However the high cost and technical problems of manufacturing large optical components will set a limit to this approach.

An alternative method to prevent ground state depletion is the addition of buffer gases to remove the vibrational bottleneck by collisional energy transfer.

In this paper, the requirements for selection of suitable buffer gases are discussed and an experimental and numerical study of the influence of these additives on the performance of the 385 μm optically pumped D_2O laser is presented.

II. THEORY

The optically pumped D_2O laser has been investigated extensively both in theory [2] and experiment [3], [4]. In particular it has been shown that the far infrared emission at 385 μm is due to a stimulated Raman process, during which the D_2O molecules are excited to the ν_2 vibrational state by the 9R(22) line of the CO_2 laser. Fig. 1 shows a simplified diagram of the energy levels involved. Apart from the optical transitions, the description of the dynamics of optical pumping has to include molecular relaxation processes. Within the rotational sublevels of each vibrational state the equilibrium population is reestablished on a very fast time scale (typically 8 ns•Torr), whereas the relaxation of the vibrational levels is slower by several orders of magnitude. The energy of the molecules excited to the ν_2 vibrational state has to be transferred by molecular collisions to translational and rotational degrees of freedom. For the ν_2 vibrational level of D_2O a relaxation time constant of 1 μs•Torr has been measured [5]. For typical operating pressures of the D_2O laser of several Torr the relaxation time will be almost as long as the pump pulse duration. The relatively low vibrational relaxation rate causes an accumulation of population in the ν_2 vibrational state and simultaneously a depletion of the ground state. This bottleneck effect leads to a decrease in absorption of the pump radiation and as a consequence to a decrease of the FIR laser gain.

It has been predicted that pump saturation may cause serious problems when attempting to achieve FIR laser pulses of 1 μs or longer [2]. During an earlier study [4] a decrease in the energy conversion efficiency of the D_2O was indeed observed when the pulse length was increased from 500 ns to 1.2 μs. The influence of the bottleneck effect on the pulse shape of an optically pumped FIR laser has been investigated by Dangoisse et al. [6]. The limitations on laser efficiency due to a bottleneck effect are already well known from studies of the CO_2 laser [7], [8].

As an efficient solution to the problem, buffer gas additives have been used to obtain energy redistribution via inter-molecular collisions. In the case of the CO_2 laser for instance, He atoms play

an important role in depopulating the lower laser level. Buffer gases have also been used successfully with cw FIR lasers [9,10]. Whereas in cw operation improvements can be achieved if the rate of collisional deexcitation exceeds the rate of energy transfer by diffusion to the laser tube walls, in pulsed operation energy transfer has to be established on a very much faster time scale. Since relaxation is dominated by collision processes, shorter relaxation times can of course be obtained by increasing the gas pressure. However at higher D_2O pressures, the effect of collisional broadening of the rotational levels becomes dominant and causes the FIR gain to decrease. Therefore, we seek buffer gas additives which selectively enhance the vibrational deexcitation but do not affect the lifetime of the D_2O rotational levels within the operating pressure range.

It is well known that the cross section for vibrational deexcitation can be increased by several orders of magnitude when near-resonant energy exchange is possible [11]. An efficient buffer gas molecule therefore should have vibrational levels in close proximity to the ν_2 band of D_2O. Collisional broadening on the other hand is considerably larger for molecules interacting via long range dipole-dipole forces [12]. In order to avoid this detrimental effect, buffer gas molecules without a permanent dipole moment are preferable.

Taking these points into account, we have selected buffer gas candidates according to the following guidelines :

(1)- vibrational energy levels allowing resonant energy transfer from the ν_2 level of D_2O at 1079 cm^{-1}.
(2)- negligible absorption of the pump radiation at 9.3 μm.
(3)- negligible absorption of FIR at 385 μm.
(4)- minimum collisional broadening of the D_2O rotational levels.

Resonant energy transfer only requires coincidence of the levels to within $E \simeq kT \simeq 200$ cm^{-1}, so a conflict between the requirements (1) and (2) can be avoided. Furthermore, molecules may be considered for which the particular vibrational transition is not infrared active. If we choose molecules which have no permanent dipole moment and therefore have no far infrared active rotational transitions, criteria (3) and (4) can be satisfied simultaneously.

III. NUMERICAL SIMULATION

A numerical simulation code [13] has been used to study the influence of a buffer gas additive on FIR output energy, pump absorption and FIR laser pulse shape. The generation of FIR radiation is described by a Raman process in a 3-level system. Both the coupling of the individual rotational levels and the vibrational relaxation into the ground state are taken into account. The corresponding time constants for D_2O are $\tau_{R,d}$ and $\tau_{V,d}$. Using a simplified model, additional relaxation rates, proportional to $1/\tau_{V,b}$ and $1/\tau_{R,b}$, are introduced to describe the vibrational deexcitation and the rotational line broadening of D_2O due to the interaction with the buffer gas molecules. For a mixture of D_2O and buffer gas at partial pressure p_d and p_b respectively, we obtain an effective relaxation time constant $\tau_{i,eff}$ by adding the rates associated with D_2O-D_2O and D_2O-buffer gas collisions :

$$\tau_{i,eff} = \frac{p_d + p_b}{p_d/\tau_{i,d} + p_b/\tau_{i,b}} \qquad (1)$$

where index i = V for vibrational relaxation,
index i = R for rotational relaxation.

During the pump pulse duration of about 1 µs the propability of multiple collisions between D_2O and buffer gas molecules is low. Therefore all buffer gas molecules are assumed to be in the vibrational ground state and the time constants for equilibration of vibrational energy within the buffer gas molecule do not have to be taken into account.

Results from the numerical simulation code for a set of parameters describing our D_2O laser (active length L=4 m; output coupling T=0.95; pump energy E_p=320 J; pulse length ~1 µs FWHM) are presented in Fig. 2. Vibrational and rotational relaxation time constants of $\tau_{V,d}$=1.5 µs·Torr and $\tau_{R,d}$=8 ns·Torr, consistent with published data [5], have been used. The three curves show the variation of FIR output energy as a function of D_2O pressure for different pumped volume cross sections A, at fixed pump energy. The laser system used during the experiments had a cross section of A=0.014 m^2. The calcula-

tions predict that the optimum operating pressure shifts to higher values and the energy conversion efficiency decreases when the pump efficiency decreases when the pump energy density is increased, indicating that pump saturation is important.

For the intermediate case in Fig. 2 ($A=0.014\ m^2$) the effect of a buffer gas additive on the FIR output energy has been investigated.

The influence of each of the two parameters $\tau_{V,b}$ and $\tau_{R,b}$ characterizing the buffer gas has been studied separately. The parameters describing the D_2O laser are identical to those of Fig. 2 for the case with $A=0.014\ m^2$. The results of the calculations are presented in Figs. 3(a) and (b) which show the variation of FIR pulse energy when the total pressure is increased by adding buffer gas to a starting pressure of 4.0 Torr of D_2O. The curve describing operation in pure D_2O is included for comparison (solid line). In Fig. 3(a), $\tau_{R,b}$ has been chosen to be the same as $\tau_{R,d}$, the corresponding parameter for D_2O-D_2O collisions. The results of Fig. 3(b) are obtained for $\tau_{R,b} = 5 \cdot \tau_{R,d}$, thus assuming a weaker broadening of the D_2O rotational level by interaction with the buffer gas molecules. For both sets of curves $\tau_{V,b}$ was varied from 0.5 $\mu s \cdot$Torr to 2.0 $\mu s \cdot$Torr, covering the range of values smaller and larger by a factor of two than the corresponding parameter for D_2O-D_2O collisions.

Comparing Figs. 3(a) and (b), it can be seen that $\tau_{R,b}$ determines the behavior at high partial pressures of buffer gas, whereas $\tau_{V,b}$ is most important at low partial pressures. In particular for the case of $\tau_{R,b} = \tau_{R,d}$, an increase in FIR energy can only be obtained if $\tau_{V,b} < \tau_{V,d}$. When however $\tau_{R,b} > \tau_{R,d}$, as in Fig. 3(b), higher partial pressures of the buffer gas can be used and even molecules with $\tau_{V,b} \gtrsim \tau_{V,d}$ allow us to obtain higher pulse energies than with pure D_2O.

From the results of the numerical simulation, it is concluded that for an efficient buffer gas the criteria (1) and (4) are equally important. For vibrational and rotational time constants which are of the same order of magnitude as those quoted for D_2O-D_2O collisions, a noticeable increase in the efficiency of a high power D_2O laser can be expected.

IV. EXPERIMENTAL

a) Choice of molecules

Several molecules have been investigated as a test for some of the selection guidelines given above. Table I lists the molecules together with their vibrational energy levels close to the ν_2 band of D_2O (1079 cm^{-1}) and their static electric dipole moments p_s.

The molecules that produced an increase (+) in FIR output energy when used as additives in a pulsed D_2O laser (i.e. SF_6, CF_4 and n-hexane) all satisfy the selection criteria and were studied in more detail. Sulphur hexafluoride (SF_6) and carbon tetrafluoride (CF_4) are spherical top molecules which possess neither permanent electric dipole nor quadrupole moments. The linear molecule n-hexane (C_6H_{14}) has a large number of vibrational degrees of freedom with several vibrational bands in the region of interest. Both molecules C_6H_{16} and SF_6 have already been reported as efficient buffer gases in a cw CH_3F laser [9,10]. For each of the three molecules, absorption on the 9R(22) line of the CO_2 laser was measured using the FIR laser tube as an absorption cell. The absorption of SF_6 was at least an order of magnitude lower than that of D_2O and the absorption of CF_4 [16], [17] and C_6H_{14} were negligible.

b) Experimental details

The CO_2 laser used as optical pump for the D_2O laser comprises a hybrid TEA laser oscillator operating in a single mode on the 9R(22) line and an electron-beam preionized amplifier, as represented in Fig. 4.

The oscillator is identical to that in an earlier publication [4], whilst the e-beam amplifier is now used without preamplifier in a more efficient triple-pass configuration. In order to achieve high gain on the 9R(22) line, a relatively CO_2-rich gas mixture of CO_2:N_2:He = 4:1:1 is used at a total pressure of 2.3 to 2.6 atm. Between the first and second passages a grating, G_2, with 150 rulings per mm is used in first order to prevent parasitic oscillation on any

line other than 9R(22) from propagating backwards into the oscillator. The total optical path length from the CO_2 laser oscillator to the FIR resonator is 65 m.

With careful adjustment of the time delay between the firing of the oscillator and the amplifier, the system is capable of producing single mode pulses of 1 μs FWHM with energy up to 850 J.

The FIR laser (Fig. 5) comprises a 4.0 m long folded unstable resonator formed by a concave mirror (M_{CC}, radius of curvature 10.3 m, diameter 200 mm) and a convex mirror (M_{CV}, radius of curvature 2.3 m, diameter 42 mm). The resonator is folded by a wire grid (W) which is 90% transmitting for the pump beam and 75% reflecting for the FIR. For this configuration an effective output coupling of T=0.95 has been calculated. The pump beam from the CO_2 laser enters the tube via a 180 mm diameter KCl window (K). The glass tube (T) serves to confine the CO_2 laser radiation to the volume of the FIR resonator. The limiting aperture of the FIR laser is 200 mm. An off-axis paraboloidal mirror (Mp) is used to collect and focus the FIR beam to a point outside the tube. Because the FIR resonator does not contain any mode selective elements, the laser pulses show modulation due to mode beating.

c) Results

(1) Pump saturation.

In Fig. 6 the FIR pulse energy is plotted versus the pulse energy of the CO_2 pump laser for operation at a filling pressure of 4.0 Torr of D_2O. Deviations from a linear relationship become noticeable at pump energies of about 150 J (energy densities of ~10 kJ/m^2). With the addition of 16.0 Torr of SF_6 (upper curve) these saturation effects disappear. The influence of the buffer gas SF_6 on the absorption of the pump radiation is shown in Fig. 7. The fraction of unabsorbed pump pulse energy is plotted as a function of total pressure with the D_2O partial pressure kept fixed at 4.0 Torr and SF_6 added. The pump beam absorption is clearly increasing with SF_6 pressure as is expected from our model for a buffer gas that permits efficient vibrational deexci-

tation of the D_2O molecules. The numerical code predicts a similar behavior (solid curve) although no attempt has been made to fit these experimental results. This observation seems to be at variance with the results presented in [10] for a cw CH_3F laser. However it should be noted that an increase in absorption induced by the addition of buffer gas can only be expected if the vibrational bottleneck effect causes strong saturation of the pump transition as is the case for the pulsed D_2O laser operated under the conditions described above. As already mentioned above, the absorption of the 9R(22) line of the CO_2 laser in pure SF_6 in this pressure range is small enough to be neglected.

(2) FIR pulse energy.

The effects of the candidate buffer gases on the D_2O laser output were investigated by measuring the variation of pulse energy with total pressure for D_2O alone and for various mixtures of D_2O and buffer gas. Fig. 8(a) shows the results of such a set of measurements for the buffer gas SF_6. Each point is the average of at least three shots, and the curves are least square fits to the data. The points fitted by the solid curve in Fig. 8(a) show the FIR pulse energies with pure D_2O. The other curves represent the pulse energies for a fixed D_2O partial pressure, as indicated, the total pressure being varied by progressively adding SF_6. The CO_2 laser pump energy entering the D_2O laser was 320 J, in a 1 μs long pulse. For an effective pumping beam area of A=0.012 m^2 the spatially averaged energy density is 27 $kJ \cdot m^{-2}$.

Fig. 8(b) shows results of the numerical simulation code produced by adjusting parameter values to obtain good agreement with the experimental results for SF_6. Apart from a constant scaling factor for the FIR pulse energy, there is good qualititive agreement between the results given in Figs 8(a) and (b), which confirms the model of the D_2O-buffer gas interaction. The parameter values for SF_6 and CF_4 as obtained from the fitting procedure are summarized in Table II.

Because the model used in the simulation code is of necessity a simplification of the real laser system, for example in its assumption of spatially uniform pumping, it is not reasonable to expect to obtain precise numerical values for the fitted parameters. Rather, the purpose of performing the fit is to obtain information about the relative values of the time constants.

The best fit value of the effective beam area A=0.014 m^2 is in good agreement with the value 0.012 m^2 which was estimated with a large uncertainty from CO_2 laser burn marks on thermally sensitive paper. The parameter $\tau_{R,d}$ was kept fixed at the published value of 8 ns•Torr [18]. The best fit value $\tau_{V,d}$=1.5 μs•Torr, whilst somewhat larger than the published value of 1.0 μs•Torr [5], is not unreasonable given the limitations of the code.

The most interesting information obtained from the simulation comes from a comparison of D_2O and buffer gas parameter values. It is found that the vibrational relaxation time constant for buffer gas-D_2O collisions, $\tau_{V,b}$ is not very different from the value for D_2O-D_2O collisions, $\tau_{V,d}$=1.5 μs•Torr. The difference between $\tau_{V,b}$ values for SF_6 and CF_4 reflects the faster increase in FIR energy with increasing partial pressure for CF_4 than for SF_6, at low partial pressures. The closeness of the values of $\tau_{V,b}$ and $\tau_{V,d}$ means that the buffer gases are about as effective as D_2O itself in deexciting the ν_2 vibrational level of D_2O.

In order to explain why, at D_2O pressures near 4 Torr, the addition of buffer gas is more beneficial to laser efficiency than the addition of further D_2O, it is necessary to compare the rotational relaxation time constants $\tau_{R,d}$ and $\tau_{R,b}$. We see that $\tau_{R,b}$= 46 ns•Torr (for both SF_6 and CF_4) is considerably larger than the corresponding D_2O time constant $\tau_{R,d}$=8 ns•Torr. The addition of buffer gases therefore contributes much less to the detrimental rotational line broadening than would the addition of the same quantity of D_2O. Since $\tau_{V,d}$ and $\tau_{V,b}$ are about equal, a higher relaxation rate is achieved via a sufficiently high partial pressure of the buffer gas.

Caution must be employed in interpreting the quoted values of $\tau_{R,b}$, since the fit is quite insensitive to the precise value. A reasonable fit of the model to the observed data can be obtained with a large range of values as long as the condition $\tau_{R,b} \gg \tau_{R,d}$ is satisfied.

Fig. 8(c) shows a comparison of the performance of the D_2O laser with SF_6 and n-hexane for a D_2O pressure of 4.0 Torr (which is not far from the optimum D_2O pressure for both buffer gases). These results were obtained with a beam reducing telescope which increased both the CO_2 beam transport efficiency and the pump energy density in the D_2O laser. The 2.6 J pulses are the most energetic that have been obtained from this laser. Higher pulse energies from a D_2O laser have so far only be reported in [19]. The different pressure dependence for the two buffer gases indicates that n-hexane has smaller $\tau_{V,b}$ and $\tau_{R,b}$ than SF_6.

(3) Pulse shape.

Observation of the D_2O laser pulse shape clearly shows the influence of the bottleneck effect. The accumulation of D_2O molecules in the ν_2 vibrational state should be observable as a decrease in the energy conversion efficiency after a time of the order of one or two vibrational relaxation time constants.

In Fig. 9 the top and middle traces are measured CO_2 laser and FIR laser pulses respectively. The bottom traces are calculated FIR pulse shapes with the actual CO_2 laser pulse as input. For the purpose of comparison with the numerical results, the modulation on the recorded FIR pulses due to mode beating has been filtered out. It can be seen that the FIR power (middle trace) falls more rapidly than the pump power (top trace), beginning about 0.4 μs after the start of the pulse, for a laser operated with 4.0 Torr of pure D_2O. The 0.4 μs delay in the onset of the dip is consistent with the estimated value of $\tau_{V,d}/P_{tot}$.The simulation code predicts a FIR pulse shape (bottom trace) which is in qualitative agreement with the observed pulse. The simulated pulse differs from the observed one mainly in having a smaller bottleneck dip. Addition of 4.0 Torr of SF_6 (Fig. 9(b)) is seen to reduce the size of the bottleneck dip and with 16.0

Torr there is no evidence of it any more. In the latter case, the FIR pulse shape is essentially identical to that of the pump, in agreement with the theoretical predictions.

(4) Optimization of buffer gas performance.

Noting that for near optimum partial pressure of D_2O the FIR pulse energy is almost independent of total pressure in the range above 10 Torr (see Fig. 8), we determined the optimum D_2O partial pressure in a more precise way. For this purpose the FIR pulse energy was measured as a function of D_2O partial pressure for fixed total pressure, by varying the mixing ratio of D_2O and buffer gas.

Fig. 10 shows the results of such measurements for SF_6 (P_{tot}= 17.0 Torr) and CF_4 (P_{tot}=12.0 Torr), together with the curve predicted by the code using the parameter values for CF_4 (solid line). The results from the numerical code have been scaled in order to obtain the same peak height as in the experiment. It is seen that under the operating conditions employed, the optimum partial D_2O pressure is between 3.5 and 3.8 Torr for CF_4 and SF_6. The code, whilst agreeing with the general form of the experimental curves predicts a somewhat higher value.

Table III summarizes the improvements in FIR output energy with the three buffer gases.

V. CONCLUSIONS

An experimental study supported by numerical simulations has been carried out to investigate the influence of buffer gas additives on output energy and pulse shape of an optically pumped D_2O laser.

The molecules that were found to increase the pumping efficiency are characterized by near-resonant vibrational levels allowing fast vibrational energy exchange, and by lack of a permanent dipole moment to avoid broadening of the D_2O rotational levels.

The experiments were performed using a single mode CO_2 laser providing pump energies up to 850 J in 1 μs long pulses. Under optimum conditions, FIR emission of 2.6 J per pulse has been measured.

At pump energy densities, which in pure D_2O would lead to saturation caused by the vibrational bottleneck, an increase in pulse energy of up to 40% has been observed using SF_6, C_6H_{14} or CF_4 as a buffer gas additive. The observed dip in the FIR pulse shape during long pump pulses in pure D_2O is filled in when buffer gas is added. This important effect permits long pulse operation.

As for the design of a D_2O laser with specified output energy, the use of a buffer gas as a means to avoid pump saturation will considerably reduce the required laser volume.

ACKNOWLEDGEMENTS

The authors gratefully acknowledge the advice of Dr. H. Van den Bergh in the selection of buffer gas molecules. They also thank Q.H. Do for his assistance during some of the experiments.

REFERENCES

[1] D.E. Evans, L.E. Sharp, W.A. Peebles and G. Taylor, "Far-Infrared Super-Radiant Laser Action in Heavy Water", Opt. Commun. 18, 479 - 484 (1976)

[2] R.J. Temkin, "Theory of Optically Pumped Submillimeter Lasers", IEEE J. Quantum Electron. QE-13, 450 - 454 (1977)

[3] P. Woskoboinikow, H.C. Praddaude, W.J. Mulligan, D.R. Cohn and B. Lax, "High-Power Tunable 385 μm D_2O Vapour Laser Optically Pumped with a Single-Mode Tunable CO_2 TEA Laser", J. Appl. Phys. 50, 1125 - 1127 (1979)

[4] R. Behn, I. Kjelberg, P.D. Morgan, T. Okada and M.R. Siegrist, "A High Power D_2O Laser Optimized for Microsecond Pulse Duration", J. Appl. Phys. 54, 2995 - 3002 (1983)

[5] R.L. Sheffield, K. Boyer and A. Javan, "Study of Vibrational and Rotational Relaxations in D_2O", Optics Lett. 5, 10 - 11 (1980)

[6] D. Dangoisse, P. Glorieux and J. Wascat, "Diffusion and Vibrational Bottleneck in Optically Pumped Submillimeter Lasers", Int. J. Infrared and Millimeter Waves 2, 215 - 229 (1981)

[7] P.K. Cheo, "Effects of CO_2, H_e, and N_2 on the Lifetimes of the 00^01 and 10^00 CO_2 Laser Levels and on Pulsed Gain at 10.6 μm", J. Appl. Phys. 38, 3563 - 3569 (1967)

[8] P.K. Cheo, "CO_2 Lasers", p. 148 - 167 in "Lasers", vol. 3, edited by A.K. Levine and A.J. DeMaria, M. Dekker, New York (1971)

[9] T.Y. Chang and C. Lin, "Effects of Buffer Gases on an Optically Pumped CH_3F FIR Laser", J. Opt. Soc. Am. 66, 362 - 369 (1976)

[10] N.M. Lawandy and G.A. Koepf, "Energy-Transfer-Mechanisms in the CH_3F-SF_6 Optically Pumped Laser", Opt. Lett. 5, 336 - 338 (1980)

[11] J.D. Lambert, "Relaxation in Gases" in D.R. Bates "Atomic and Molecular Processes" Academic Press, New York, 783 - 806 (1962)

[12] P.Ch. Pandey and S.L. Srivastava, "Collision Broadening of C_2H_4O Lines. I. Broadened by Polar Molecules", J. Chem. Phys. 57, 3282 - 3286 (1972)

[13] T. Okada, R. Behn, M.A. Dupertuis, P.D. Morgan and M.R. Siegrist, "Numerical Analysis of an Optically Pumped D_2O Far Infrared Laser", J. Appl. Phys. 54, 2987 - 2994 (1983)
Note : The numerical code has been modified to include reabsorption of the 385 μm emission by a rotational transition in the ground state of D_2O.

[14] CRC Handbook of Chemistry and Physics 49th edition. The Chemical Rubber Co. Editor : R.C. Weast (1968)

[15] G. Herzberg, "Molecular Spectra and Molecular structure. Vol. 2 : Infrared and Raman Spectra of Polyatomic Molecules", Van Nostrand, Princeton (1945)

[16] DMS Tables, Edited by : Inst. f. Spektrochemie u. Angewandte Spektroskopie, Dortmund, and Infrared Absorption Data Joint Committee, London, Butterworths Scientific Publ., London

[17] J.J. Tiee and C. Wittig, "CF_4 and NOCl Molecular Laser Operating in the 16 μm Region", Appl. Phys. Lett. 30, 420 - 422 (1977)

[18] S.J. Petuchowski, A.T. Rosenberger and T.A. DeTemple, "Stimulated Raman Emission in Infrared Excited Gases", IEEE J. Quantum Electron. QE-13, 476 - 481 (1977)

[19] A. Semet, L.C. Johnson and D.K. Mansfield, "A High Energy D_2O Submillimeter Laser for Plasma Diagnostics", Int. J. Infrared and Millimeter Waves 4, 231 - 246 (1983)

FIGURE CAPTIONS

Fig. 1

Schematic diagram of D_2O energy levels. Pump process (1) leads to a laser and (2) to a stimulated Raman transition at 385 μm. Relaxation of the vibrational excitation can occur either via conversion to translational and rotational energy (3) or via transfer of energy to a buffer gas molecule with a vibrational level close to that of D_2O (4).

Fig. 2

Results from the numerical simulation code showing FIR output energy as a function of D_2O pressure for the active volume cross sections : (a) A=0.028 m^2 (b) A=0.014 m^2 and (c) A=0.007 m^2. The time constants used in the calculations are : $\tau_{V,d}$ = 1.5 μs•Torr and $\tau_{R,d}$ = 8 ns•Torr.

Fig. 3

Calculated FIR output energies as a function of total pressure for a mixture of buffer gas and 4.0 Torr of D_2O. The buffer gas parameters are : $\tau_{V,b}$: 0.5, 1.0 and 2.0 μs Torr

$\tau_{R,b}$: 8 ns•Torr in (a)

40 ns•Torr in (b).

The results for pure D_2O are shown for comparison (solid line).

Fig. 4

Side view of CO_2 laser the system. The oscillator and the beam paths shown by broken lines lie outside the plane of the figure.

G_1 : diffraction grating for wavelength selection

A : variable apertures for transverse mode control

K : KCl windows

X : low pressure CO_2 laser module for longitudinal mode control

O : ZnSe output coupler

M : plane metal mirrors

G_2 : diffraction grating used to prevent parasitic oscillation on higher gain lines.

Fig. 5

Optically pumped FIR D_2O laser.

K : KCl window for input of CO_2 laser beam
W : Tungsten wire grid
M_{cc} : concave mirror
T : glass tube used to guide the pump beam
D : teflon sheet as beam dump for unabsorbed pump energy
M_{cv} : convex mirror
M_p : off-axis paraboloidal mirror
P : TPX window.

Fig. 6

FIR pulse energy as a function of pump pulse energy for
(a) pure D_2O, p=4.0 Torr.
(b) 4.0 Torr of D_2O and 16.0 Torr of buffer gas.

Fig. 7

Pump beam energy transmission through D_2O laser tube as a function of total pressure P_{tot} for fixed D_2O and varying SF_6 pressure. The points represent average values over three laser shots, and the solid curve gives the results from the numerical simulation using the parameters of table II.

Fig. 8

FIR pulse energy as a function of total gas pressure
(a) Experimental results with an average of 320 J of pump pulse energy, using SF_6 as buffer gas.
(b) Results of the simulation code using the SF_6 parameter values of table II, and a pump energy of 320 J.
(c) Comparison of experimental results for buffer gas additives SF_6 and n-hexane at fixed D_2O pressure of 4.0 Torr.

Fig. 9

Comparison of CO_2 and FIR laser pulse shapes. D_2O pressure : 4.0 Torr, SF_6 pressure : (a) 0 Torr, (b) 4.0 Torr and (c) 16.0 Torr.

Top : CO_2 laser pulse, experimental result,
Middle : FIR laser pulse, experimental result,
Bottom : FIR laser pulse, from simulation code.

For the observed pulses, the dots are individual samples taken by a digitizing oscilloscope.

Fig. 10

Determination of optimum D_2O partial pressure for operation with SF_6 and CF_4. The total pressure was kept constant at 17.0 Torr for the case of SF_6 and at 12.0 Torr for CF_4. The solid curve was calculated using the CF_4 parameter values of table II and has been scaled to give the same peak height as the experimental results.

Table I. Candidate buffer gas molecules.

Molecule	Permanent dipole moment p_s*	Vibrational* bands	Effect on FIR laser output
CH_3F	1.85 D	1048 cm^{-1} 1196 cm^{-1}	-
CF_4	0	904 cm^{-1} 1070 cm^{-1} 1265 cm^{-1}	+
C_2H_4	0	949 cm^{-1} 995 cm^{-1} 1050 cm^{-1} 1342 cm^{-1}	-
C_2H_3Cl	1.45 D	850-1050 cm^{-1}	-
SF_6	0	965 cm^{-1} 1262 cm^{-1} 1282 cm^{-1}	+
n-hexane C_6H_{14}	0	973-1166 cm^{-1}	+

*) Data from : [14], [15], [16].

Table II. Summary of relaxation time constants.

Parameter	Published or measured value	Best fit values SF_6	CF_4
$\tau_{V,d}$	1.0 μs•Torr	1.5 μs•Torr	1.5 μs•Torr
$\tau_{R,d}$	8 ns•Torr	8 ns•Torr	8 ns•Torr
$\tau_{V,b}$	-	1.8 μs•Torr	1.2 μs•Torr
$\tau_{R,b}$	-	46 ns•Torr	46 ns•Torr

Table III. Improvements in pulse energy using SF_6, CF_4 and C_6H_{14}.

Buffer gas molecule	SF_6	CF_4	C_6H_{14}
Maximum pulse energy (normalized)*	1.32	1.40	1.36
Optimum D_2O partial pressure (Torr)	3.8	3.5	3.0

*Note : Maximum pulse energy obtained with buffer gas additive divided by maximum energy with pure D_2O.

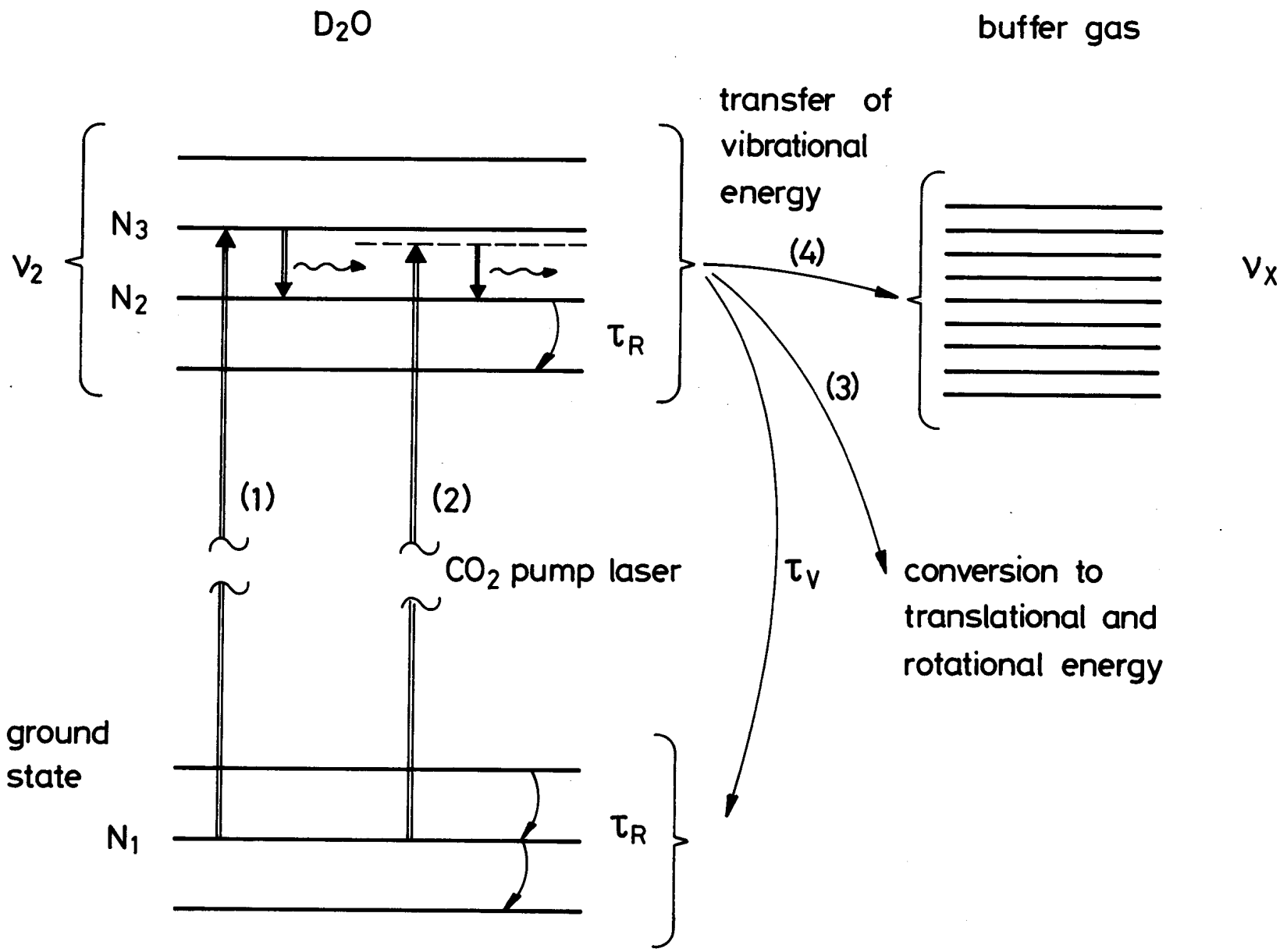
D_2O
buffer gas
transfer of vibrational energy
V_2
N_3
N_2
τ_R
(4)
V_X
(3)
(1)
(2)
CO_2 pump laser
τ_V
conversion to translational and rotational energy
ground state
N_1
τ_R

fig. 1

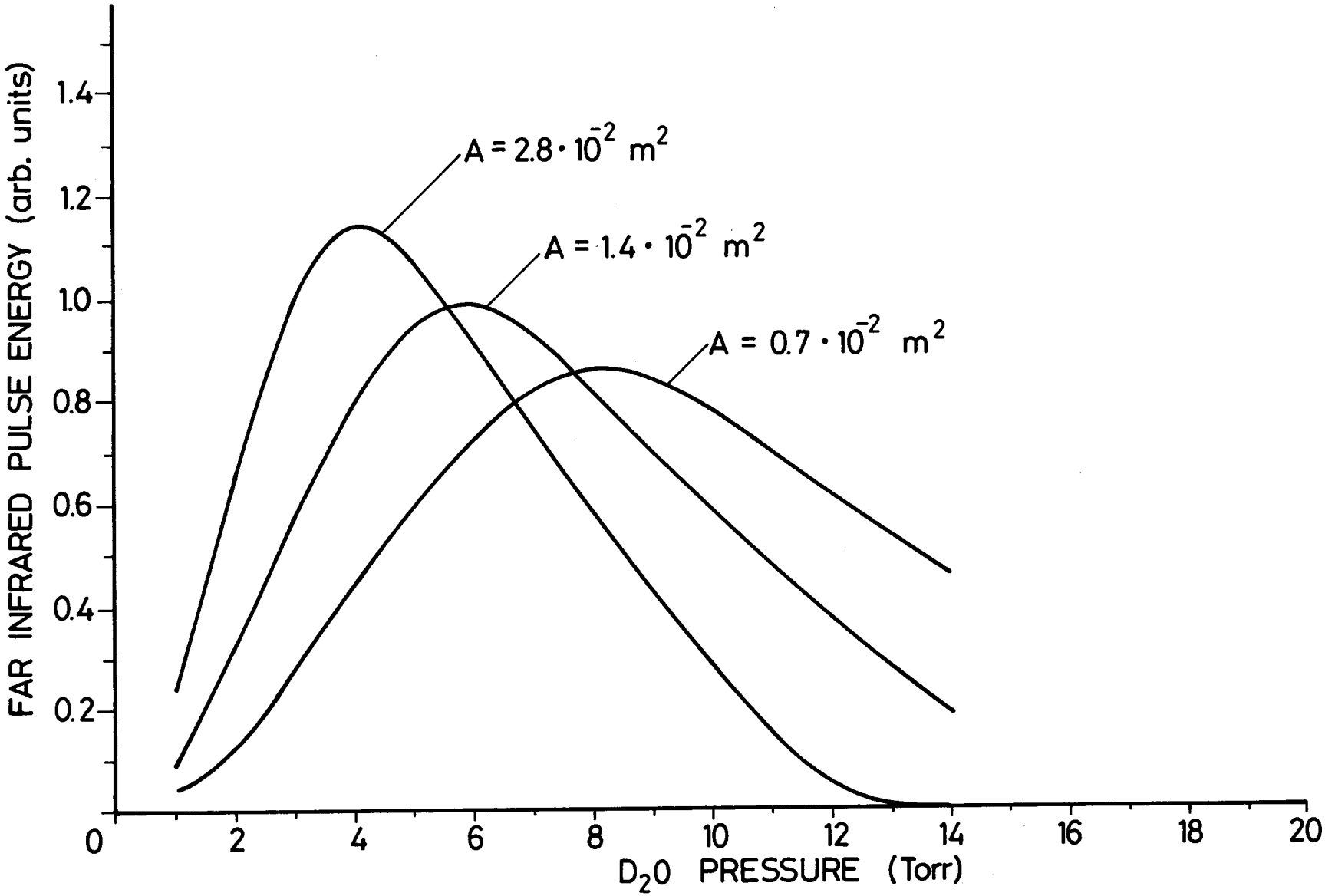
FAR INFRARED PULSE ENERGY (arb. units)
1.4
1.2
1.0
0.8
0.6
0.4
0.2
0
2
4
6
8
10
12
14
16
18
20
D_2O PRESSURE (Torr)
$A = 2.8 \cdot 10^{-2}$ m^2
$A = 1.4 \cdot 10^{-2}$ m^2
$A = 0.7 \cdot 10^{-2}$ m^2

fig.2

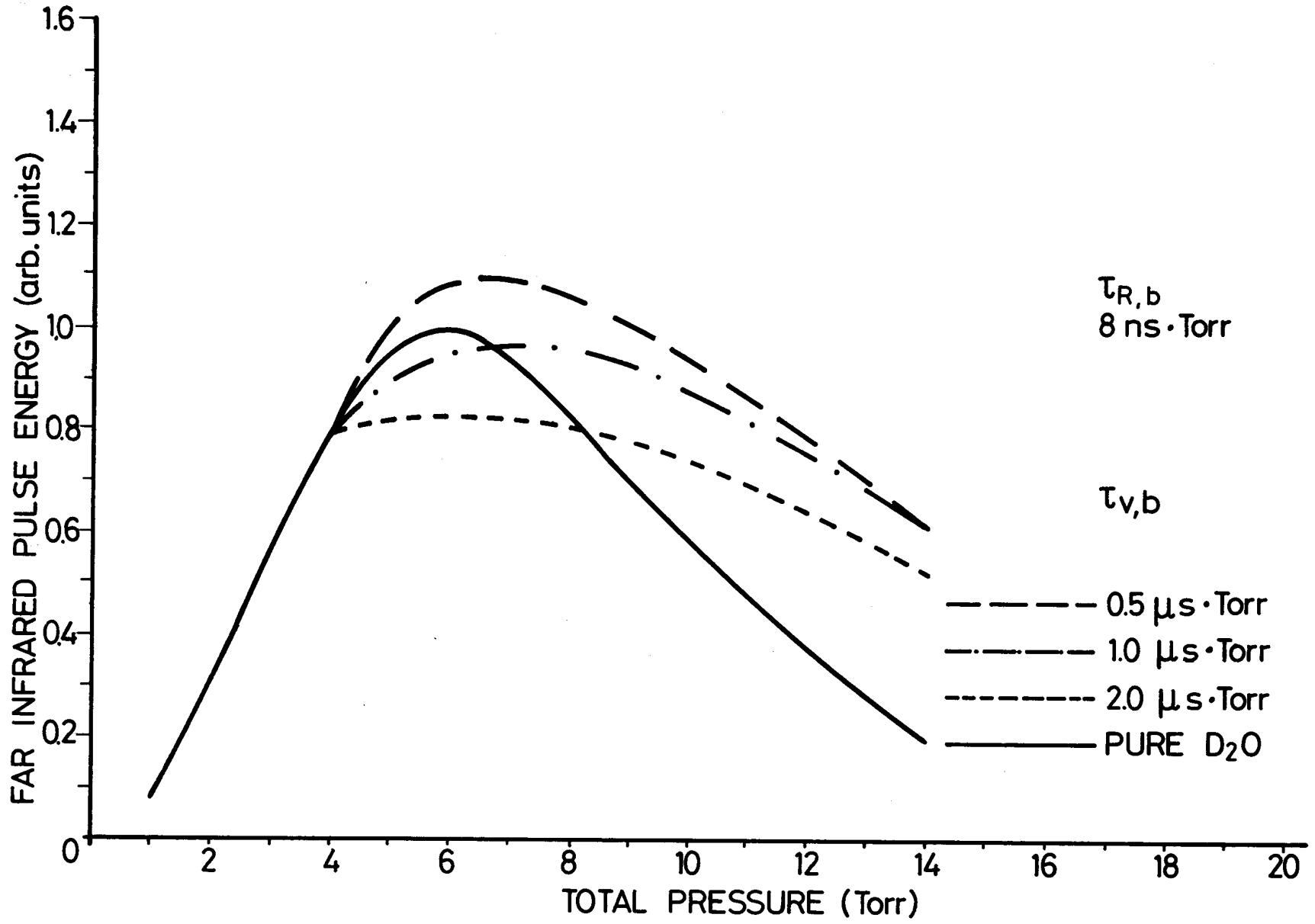
FAR INFRARED PULSE ENERGY (arb. units)
1.6
1.4
1.2
1.0
0.8
0.6
0.4
0.2
0
2
4
6
8
10
12
14
16
18
20
TOTAL PRESSURE (Torr)
τR,b
8 ns·Torr
τv,b
0.5 μs·Torr
1.0 μs·Torr
2.0 μs·Torr
PURE D2O

fig.3(a)

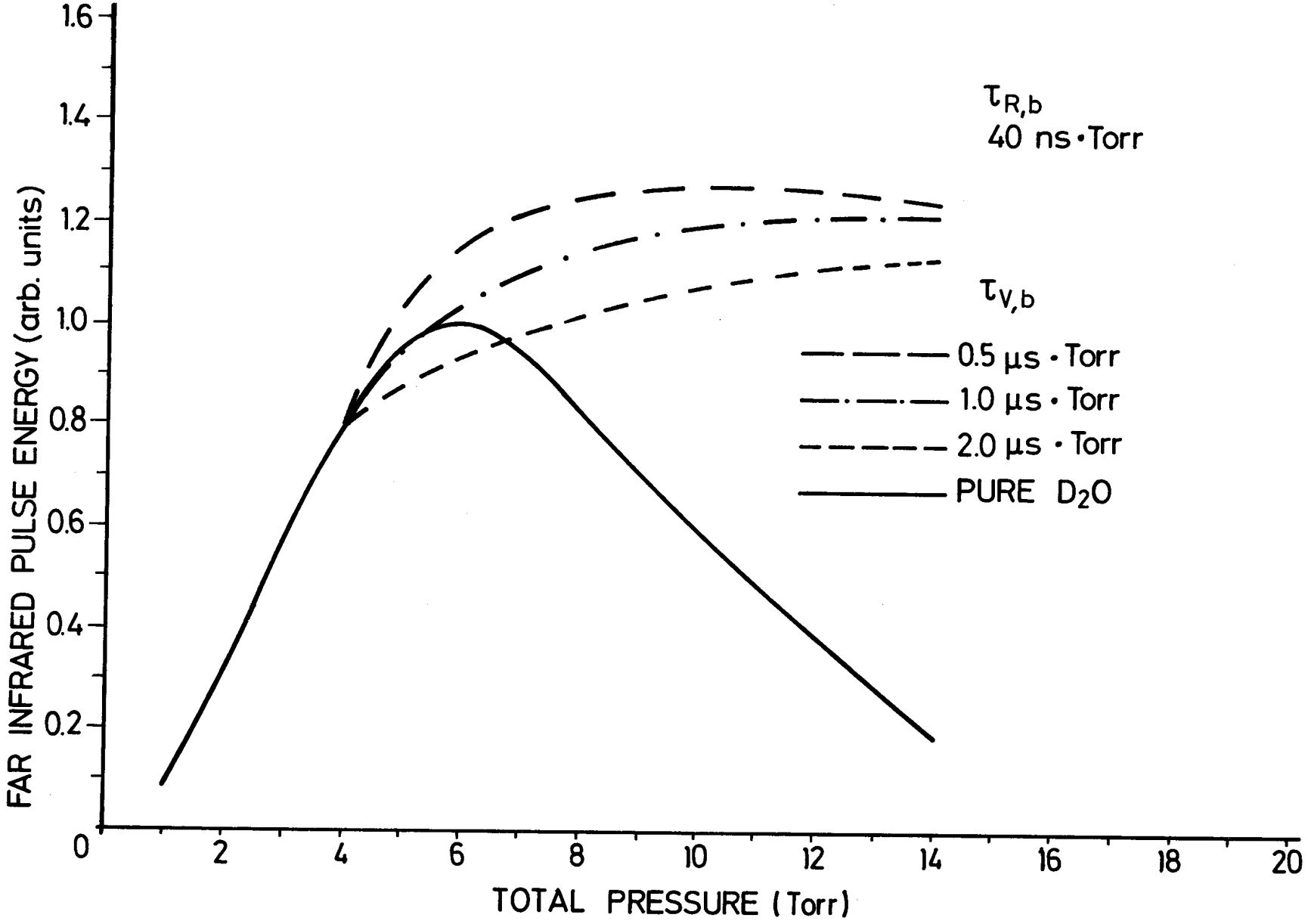
FAR INFRARED PULSE ENERGY (arb. units)
1.6
1.4
1.2
1.0
0.8
0.6
0.4
0.2
0
2
4
6
8
10
12
14
16
18
20
TOTAL PRESSURE (Torr)
$\tau_{R,b}$
40 ns·Torr
$\tau_{V,b}$
0.5 μs · Torr
1.0 μs · Torr
2.0 μs · Torr
PURE D_2O

fig.3(b)

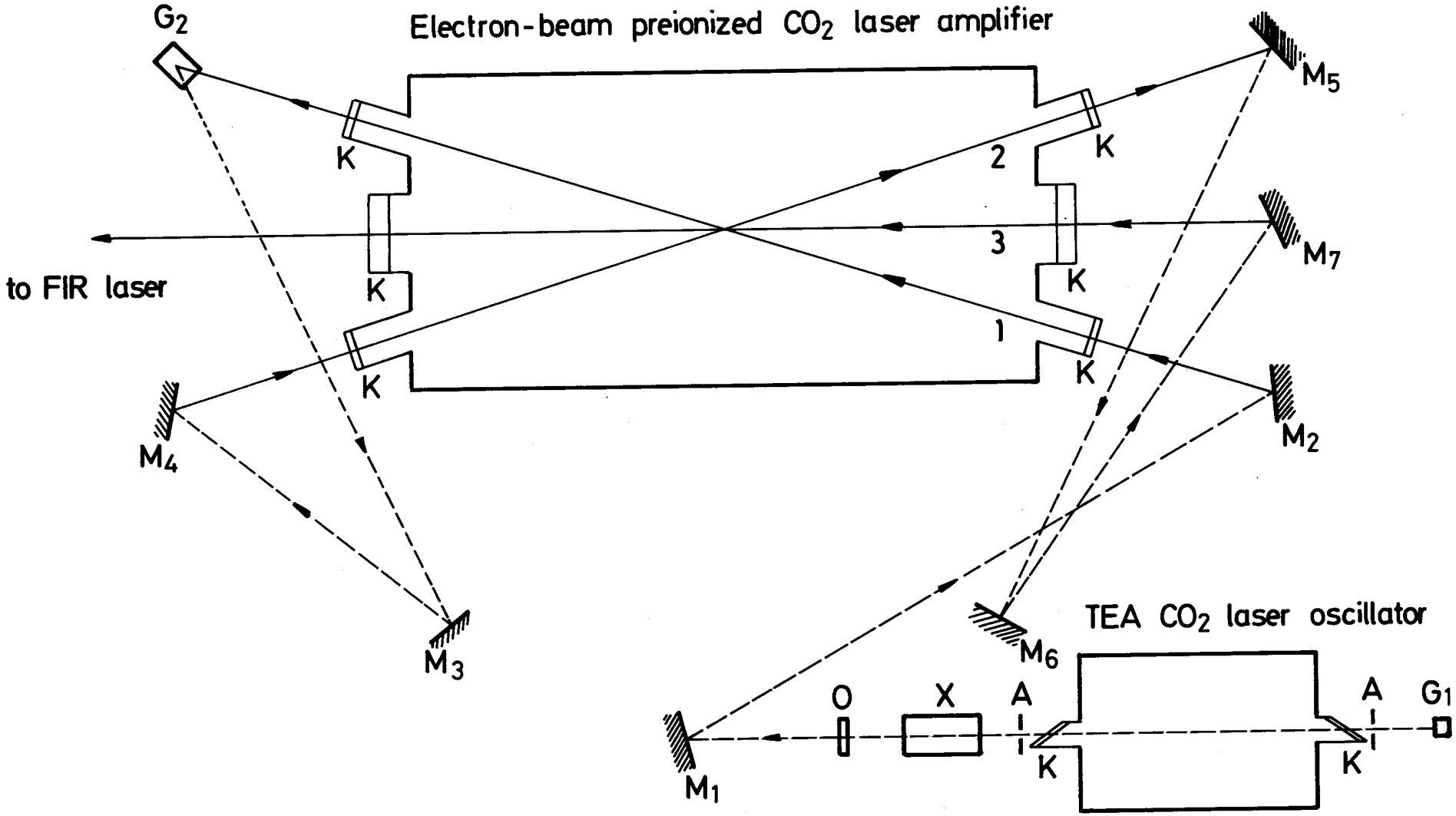
G2
Electron-beam preionized CO2 laser amplifier
M5
K
K
2
M7
3
to FIR laser
K
K
1
K
K
M4
M2
M3
TEA CO2 laser oscillator
M6
O
X
A
A
G1
K
K
M1

fig.4

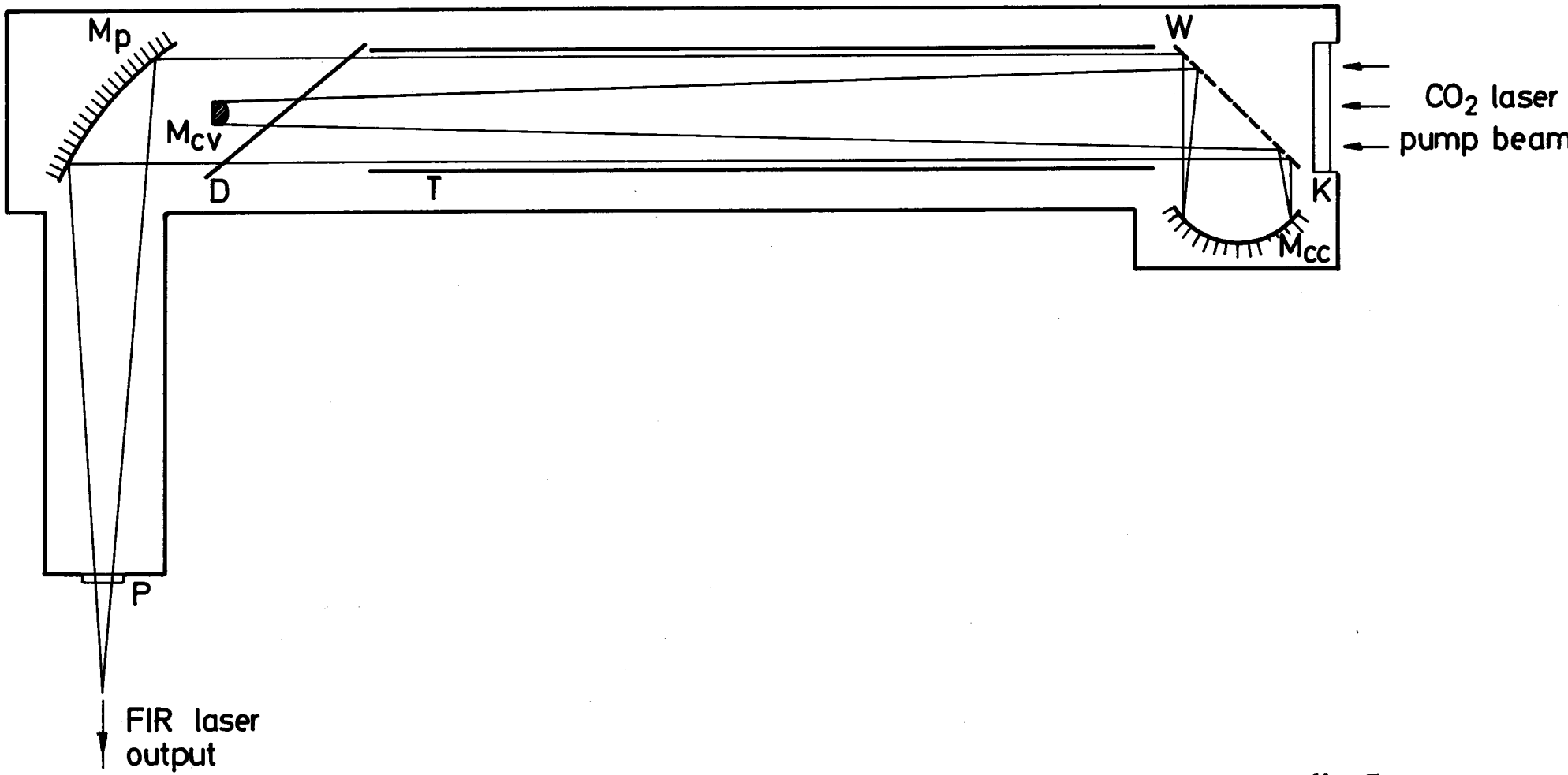

fig.5

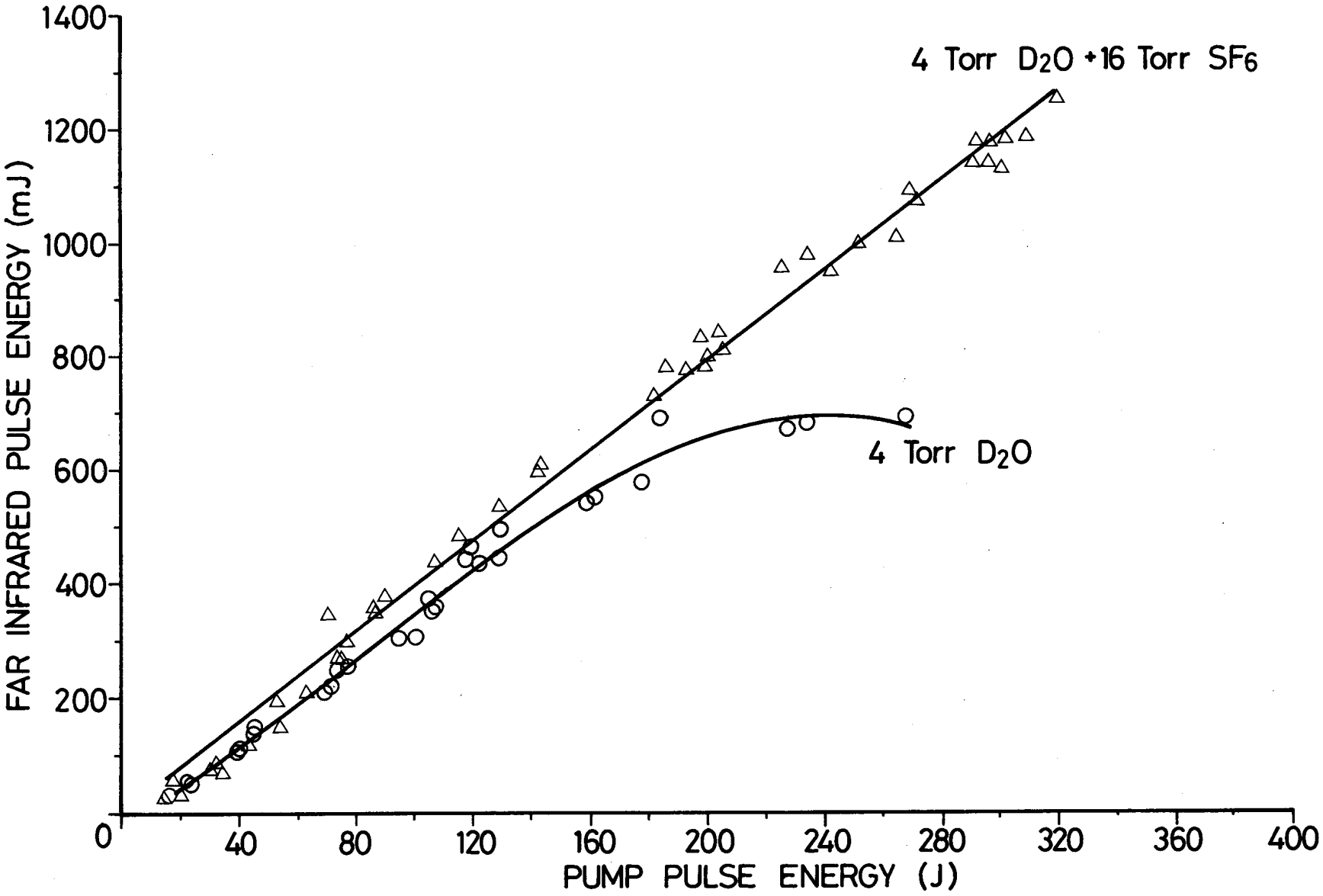
FAR INFRARED PULSE ENERGY (mJ)
1400
1200
1000
800
600
400
200
0
40
80
120
160
200
240
280
320
360
400
PUMP PULSE ENERGY (J)
4 Torr D2O +16 Torr SF6
4 Torr D2O

fig.6

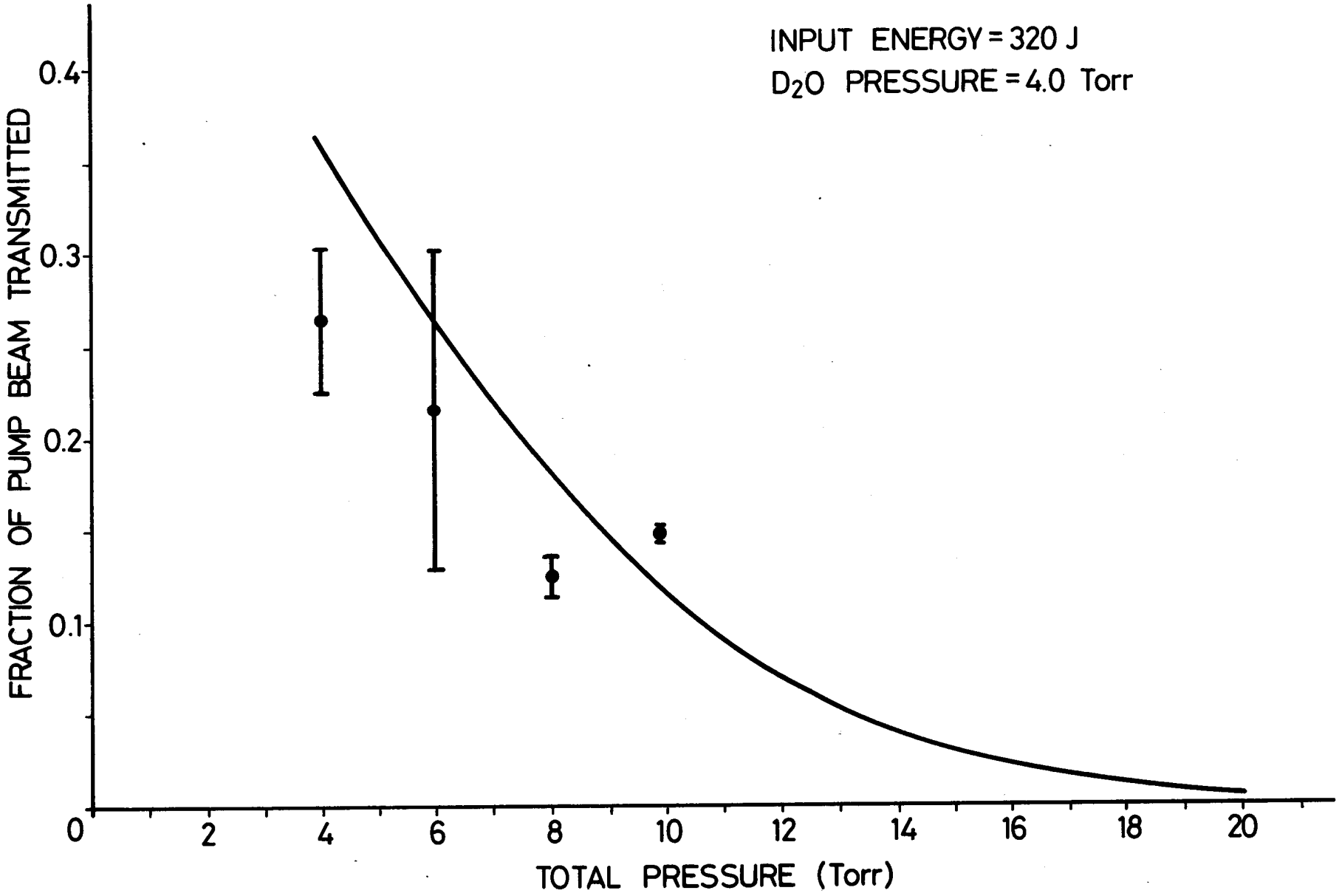
INPUT ENERGY = 320 J
D2O PRESSURE = 4.0 Torr
FRACTION OF PUMP BEAM TRANSMITTED
0.4
0.3
0.2
0.1
0
2
4
6
8
10
12
14
16
18
20
TOTAL PRESSURE (Torr)

fig.7

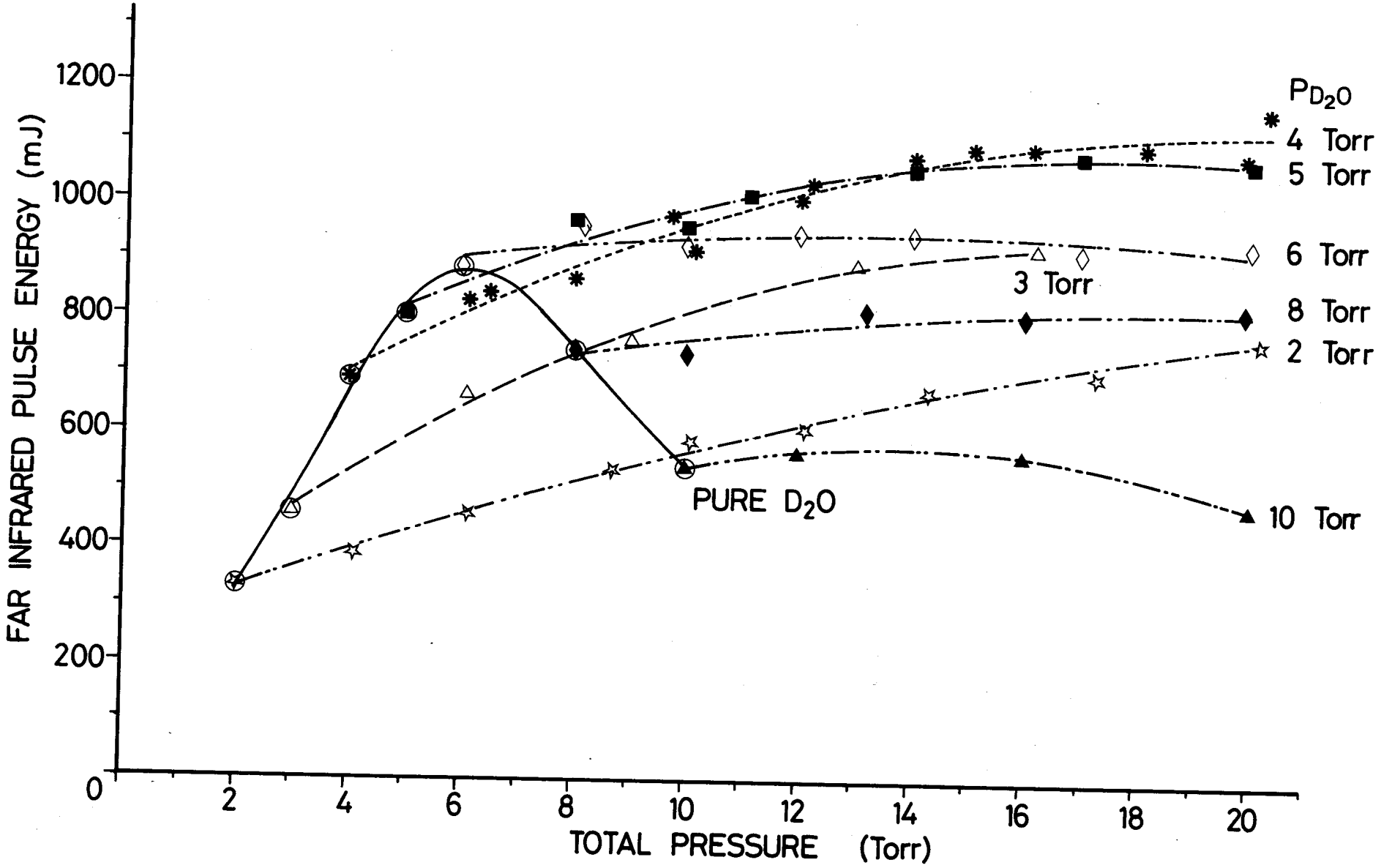
FAR INFRARED PULSE ENERGY (mJ)
1200
1000
800
600
400
200
0
2
4
6
8
10
12
14
16
18
20
TOTAL PRESSURE (Torr)
P_{D_2O}
4 Torr
5 Torr
6 Torr
3 Torr
8 Torr
2 Torr
PURE D_2O
10 Torr

fig.8(a)

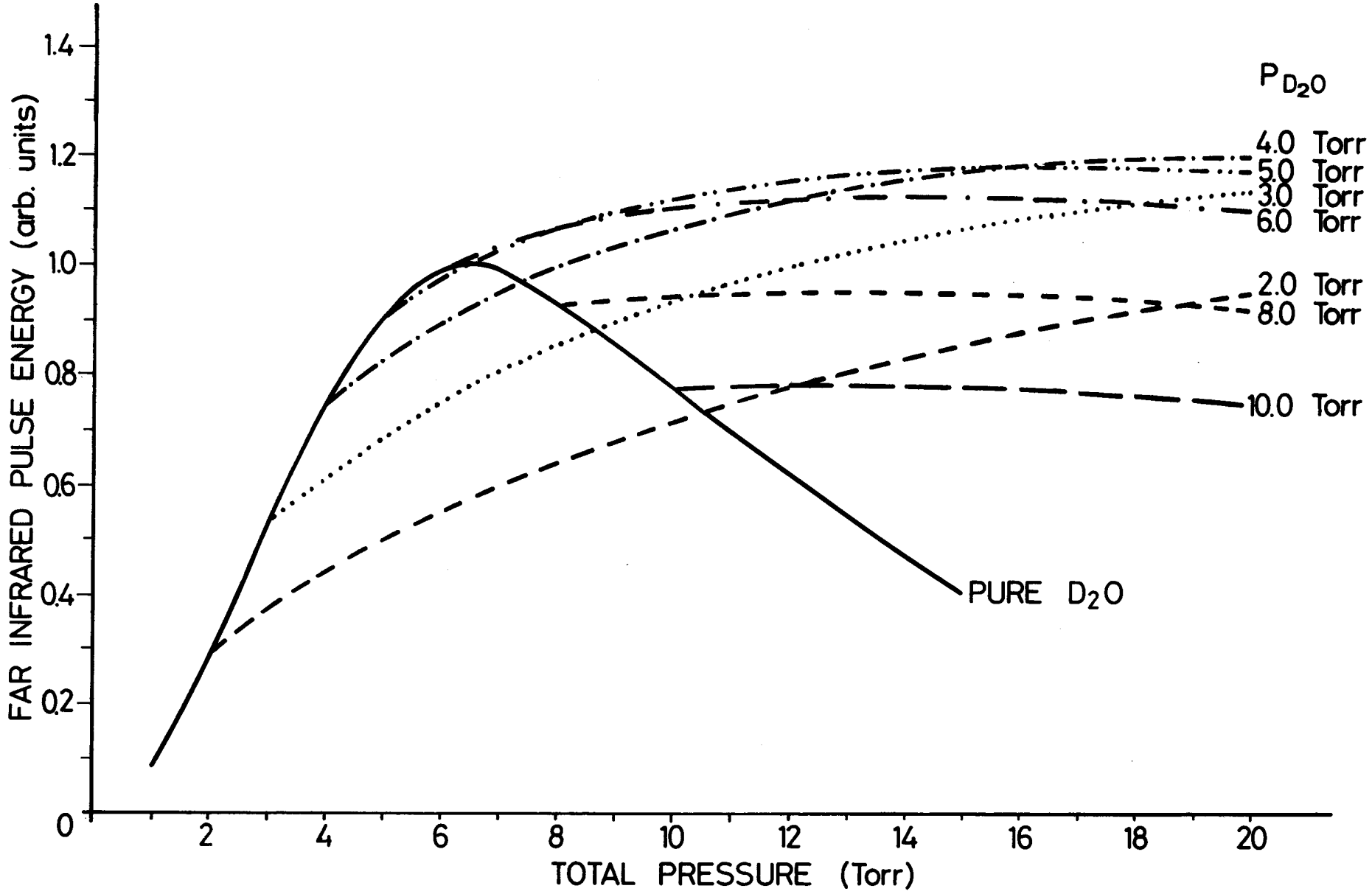
FAR INFRARED PULSE ENERGY (arb. units)
1.4
1.2
1.0
0.8
0.6
0.4
0.2
0
2
4
6
8
10
12
14
16
18
20
TOTAL PRESSURE (Torr)
P_{D_2O}
4.0 Torr
5.0 Torr
3.0 Torr
6.0 Torr
2.0 Torr
8.0 Torr
10.0 Torr
PURE D_2O

fig.8(b)

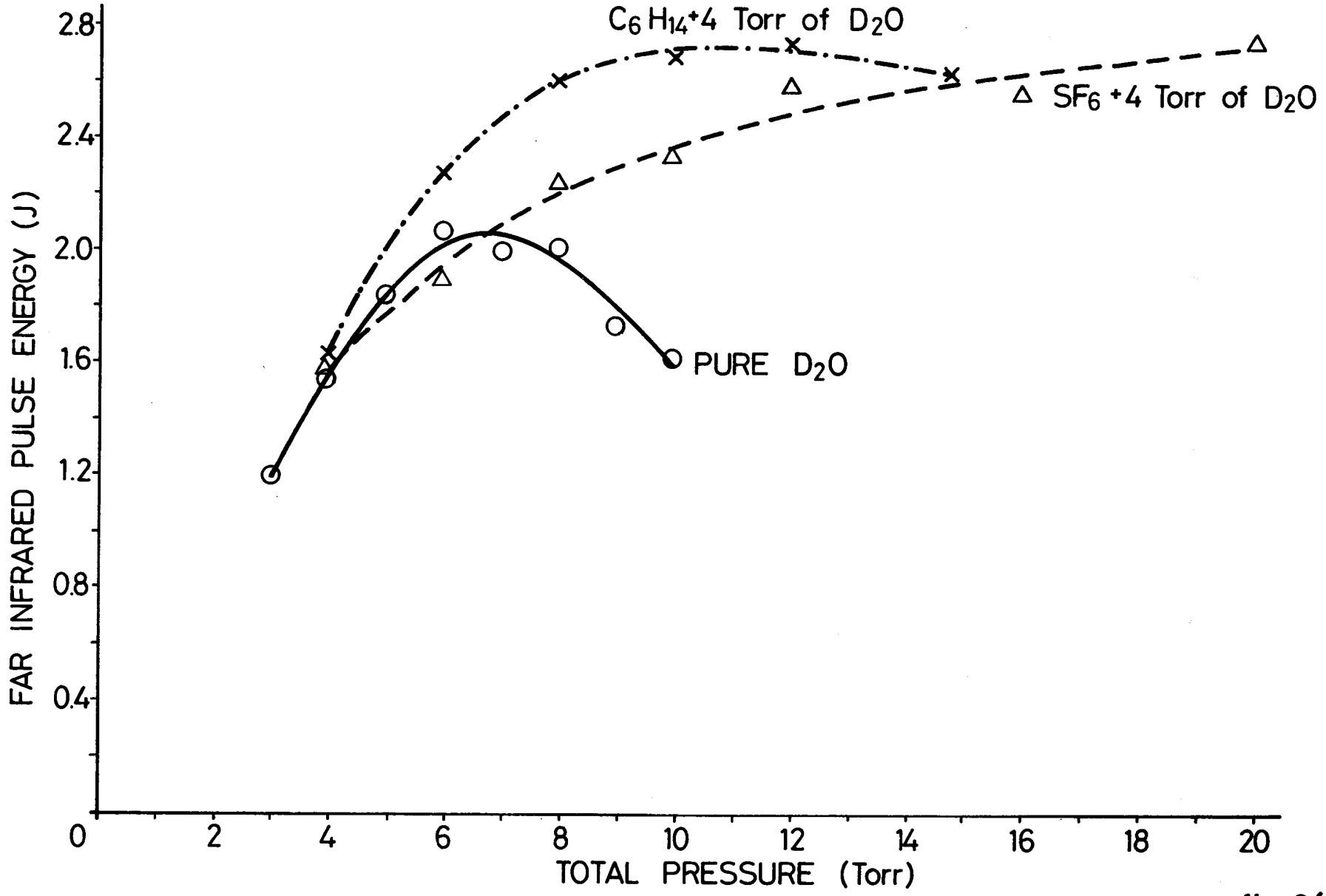
C6 H14+4 Torr of D2O
SF6 +4 Torr of D2O
PURE D2O
FAR INFRARED PULSE ENERGY (J)
TOTAL PRESSURE (Torr)
0
0.4
0.8
1.2
1.6
2.0
2.4
2.8
2
4
6
8
10
12
14
16
18
20

fig.8(c)

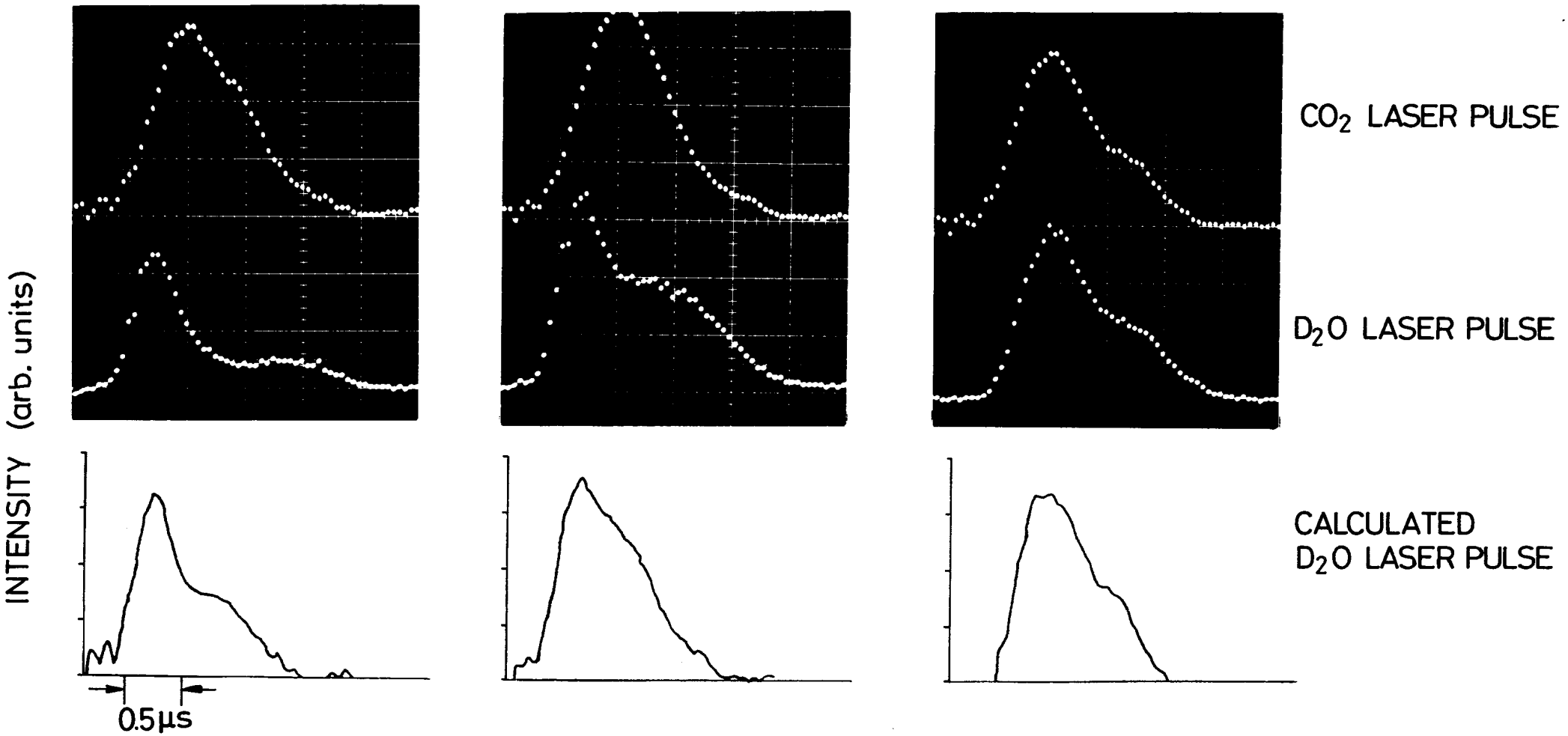
INTENSITY (arb. units)
CO_2 LASER PULSE
D_2O LASER PULSE
CALCULATED
D_2O LASER PULSE
0.5μs
(a) P_{D_2O} = 4 Torr
P_{SF_6} = 0
(b) P_{D_2O} = 4 Torr
P_{SF_6} = 4 Torr
(c) P_{D_2O} = 4 Torr
P_{SF_6} = 16 Torr

fig.9

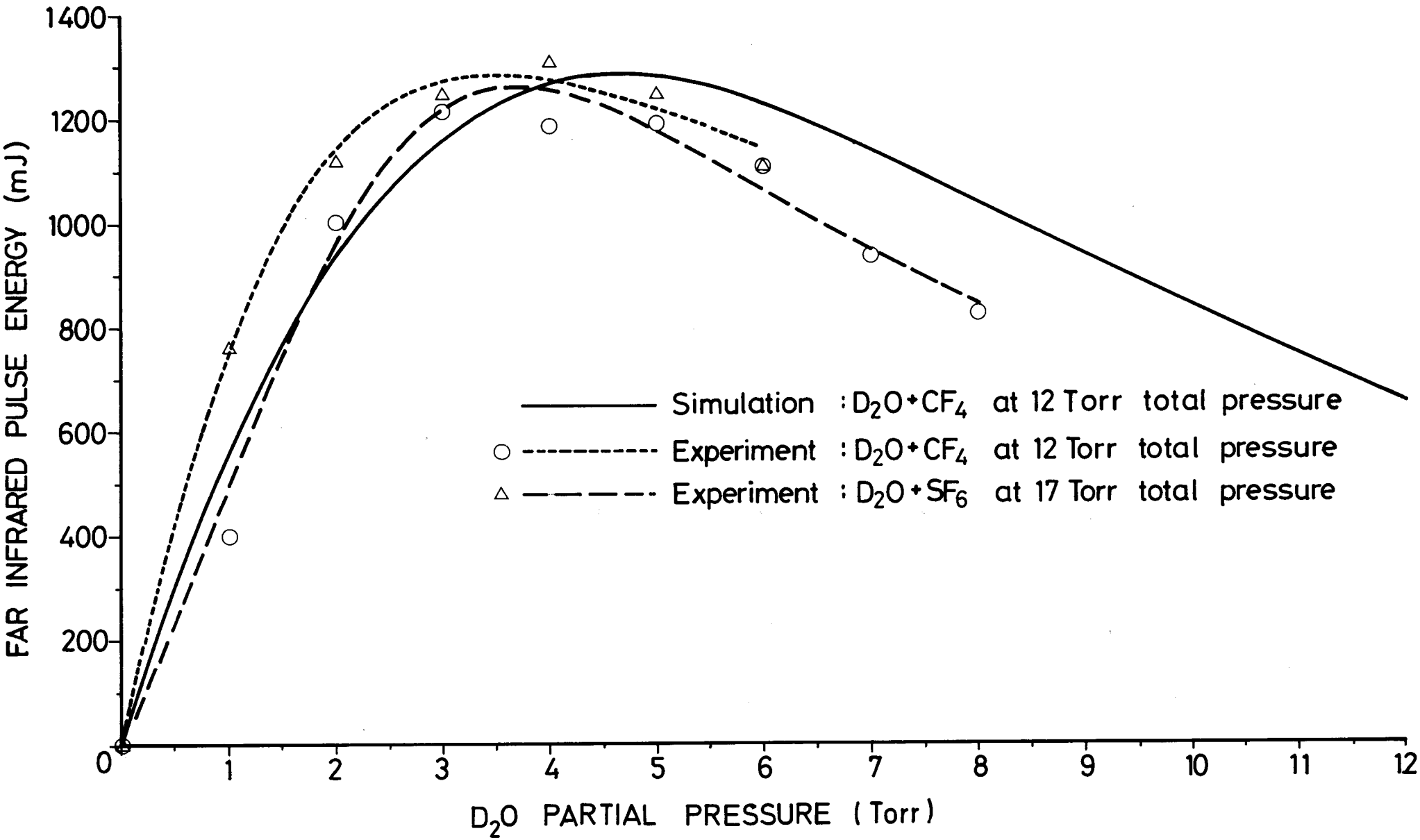
FAR INFRARED PULSE ENERGY (mJ)
1400
1200
1000
800
600
400
200
0
1
2
3
4
5
6
7
8
9
10
11
12
D2O PARTIAL PRESSURE (Torr)
Simulation : D2O+CF4 at 12 Torr total pressure
Experiment : D2O+CF4 at 12 Torr total pressure
Experiment : D2O+SF6 at 17 Torr total pressure

fig.10